Adsorption (2015) 21:321–332
DOI 10.1007/s10450-015-9671-y

Saturation loadings on 13X (faujasite) zeolite above and below the critical conditions. Part II: unsaturated and cyclic hydrocarbons data evaluation and modeling

Alaa Al Mousa[1] · Dana Abouelnasr[2,3] · Kevin F. Loughlin[2]

Received: 9 June 2014 / Revised: 3 April 2015 / Accepted: 9 April 2015 / Published online: 22 April 2015

Abstract The saturation loadings for subcritical adsorption of alkenes, aromatics and cyclic alkanes 13X zeolite are modeled using the modified Rackett model of Spencer and Danner (J Chem Eng Data 17(2):236–240, 1972) for the saturated liquid densities combined with crystallographic data for the 13X zeolite. Adsorption data from the literature is first critically evaluated and then compared to the model. Log–log plots are used to determine whether each isotherm is near saturation; isotherms that exhibit a $(\partial \ln q)/(\partial \ln p)$ slope of zero at their maximum pressure point are assumed to be saturated. For subcritical isotherms, the reduced pressure at which all isotherms became saturated is found to be relatively constant below a molecular weight of 60 g/mol, and then to decrease exponentially with molecular weight above 60 g/mol. The highest loading is used from each isotherm that approaches saturation. Unsaturated isotherms are not considered further. The theoretical equation satisfactorily models the available experimental data for the alkenes and cyclic alkanes. However, steric factors are required in the model for the aromatics. For supercritical temperatures, no model presently exists to explain the data. However, the supercritical alkene data are satisfactorily modeled with an equation of the form $q_{max} = 10 \pm 2.0$ g/100 g. There are no supercritical data for aromatic species or for cyclic alkanes.

Keywords Unsaturated hydrocarbons · Cyclic hydrocarbons · 13X zeolite · Sorbate densities · Saturation loadings · Sorbate molar volumes · Critical conditions

List of symbols

MW	Molecular weight (g/mol)
P_c	Critical pressure (kPa)
P_r	Reduced pressure
q	Zeolite loading, g/100 g zeolite crystal
q_{max}	Maximum zeolite loading, g/100 g zeolite crystal
$q_{max,c}$	Theoretical maximum zeolite loading at the critical temperature, defined by Eq. 3, g/100 g zeolite crystal
R	Gas constant, 8314 kPa-cm^3/gmol K
T_c	Critical temperature (K)
T_r	Reduced temperature
Z_{RA}	Rackett parameter

Greek letters

Γ	Normalized loading, dimensionless, calculated in Eqs. 6 and 7
ε_Z	Crystallographic 13X zeolite void fraction, 0.428 (Breck 1974, p. 133)
λ	Steric factor, the fraction of the zeolite void volume that is accessible to the sorbate. Used in Eq. 7
ρ_Z	Zeolite 13X crystallographic density, 1.43 g/cm^3, (Breck 1974, p. 133)

Kevin F. Loughlin—American University of Sharjah (retired).

Electronic supplementary material The online version of this article (doi:10.1007/s10450-015-9671-y) contains supplementary material, which is available to authorized users.

✉ Dana Abouelnasr
dabouelnasr@aus.edu

Kevin F. Loughlin
kff.loughlin@gmail.com

[1] Petrofac International Ltd, Sharjah, UAE

[2] Department of Chemical Engineering, American University of Sharjah, P.O. Box 26666, Sharjah, UAE

[3] California State University at Bakersfield, Bakersfield, USA

1 Introduction

One parameter that is common in many models for adsorption isotherms is the maximum saturation loading. In this work, we consider direct observations of saturation loadings for subcritical unsaturated hydrocarbons and for cyclic hydrocarbons on 13X zeolite. These are compared to a model that incorporates the modified Rackett model for the sorbate density combined with crystallographic information. This model was previously reported for alkanes on 5A zeolite and for alkanes on 13X zeolite (Al Mousa et al. 2014). We now consider unsaturated and cyclic alkanes on 13X zeolite. We also propose a simple model for supercritical adsorption for the alkenes. For the comparison, we collected existing adsorption data from the literature, analyzed it for consistency between studies, and used the maximum loading in each isotherm that is determined to be at or near saturation.

2 Theoretical model

The following model was previously presented in the paper of and also discussed in part one of this series (Al Mousa et al. 2014). Only pertinent equations are given here. The theoretical saturation loading of any subcritical substance in any zeolite may be calculated from first principles for zeolite crystals assuming 100 % accessibility for the alkanes, and using the modified Rackett equation for the sorbate density. The resulting model for saturation loading is:

$$q_{\max}\left(\frac{g}{100\,\mathrm{g}Z}\right) = q_{\max,c}Z_{RA}^{-(1-T_r)^{0.2857}} \tag{1}$$

where $q_{max,c}$ is the theoretical loading at critical conditions:

$$q_{\max,c} = 100\frac{\varepsilon_Z}{\rho_Z}\left(\frac{P_cMW}{RT_cZ_{RA}}\right) \tag{2}$$

ε_Z is the zeolite void fraction, and ρ_Z is the zeolite crystallographic density. Z_{RA} is a particular constant for the modified Rackett equation; values are given in the paper by (Spencer and Danner 1972). In addition, values for all the critical constants and the Rackett parameter Z_{RA} are also given on the CHERIC (2012) website.

Equation 1 may be rearranged to give a normalized value for the loading Γ by taking logarithms

$$\Gamma = (1 - T_r)^{0.2857} \tag{3}$$

where Γ is given by Eq. 4.

$$\Gamma = -\frac{\ln\left(q_{\max}/q_{\max,c}\right)}{\ln(Z_{RA})} \tag{4}$$

Using Eq. 4, the experimentally observed values for q_{max} may be plotted for all substances on a single graph, and compared to the theoretical curve, given by Eq. 3.

A theoretical plot of q_{max} versus reduced temperature calculated using Eq. 1 is presented in Fig. 1 and in Fig. S1 in the Supplementary Information for all the unsaturated and cyclic hydrocarbons used in this study. The maximum loading decreases with reduced temperature and rapidly decreases as T_r approaches 1. This is due to the increased rotational and vibrational energy of the molecules as the temperature increases.

At any particular T_r, the saturation loading generally increases with molecular size, from the smallest molecule, ethylene, to the largest molecule, 1,3-dimethylnaphthalene. The models for all the species are very similar in both shape and position, regardless of the complexity of the molecule. However, for molecules that are large or inflexible, a steric effect may arise. In these cases, a steric factor λ must be introduced into Eq. 1 giving

$$q_{\max}\left(\frac{g}{100\,\mathrm{g}Z}\right) = \lambda q_{\max,c}Z_{RA}^{-(1-T_r)^{0.2857}} \tag{5}$$

λ is a measure of the fraction of the zeolite void volume that is accessible to the adsorbate. The value of λ must be determined from the experimental data.

3 Methodology

Experimental data for isotherms of unsaturated and cyclic hydrocarbons on 13X are collected from the literature. Untabulated adsorption data on NaX, faujasite or Linde, CECA or other 13X zeolite (labelled 13X hereafter) are reported by digitizing the appropriate figures.

The data has been systematically evaluated for consistency using the nine criteria as reported in detail in Loughlin and Abouelnasr (2009).

The adsorption isotherms extracted from the literature are summarized in Table 1 for subcritical and supercritical data. The last column contains comments, including the adsorbent, the percentage binder, and the reason why a particular study might not be used. For example, (Kang et al. 2005) did not mention the % binder, and so is omitted from further consideration.

The isotherms in Table 1 are plotted by species for the purpose of evaluating their consistency. The isotherms are first considered on a q versus ln P_r plot. Inconsistent isotherms or data points are identified and removed. Isotherms passing the data consistency criteria are then plotted on a ln q versus ln P_r plot. Only isotherms which are saturated or are approaching saturation are considered further as determined by the slope of the ln q vs ln P_r plot approaching zero. Isotherms far from saturation are not included in the q_{max} observations. In addition, we also comment on the consistency of each isotherm with Henry law at low loadings $(\partial \ln q)/(\partial \ln p) = 1$ where appropriate.

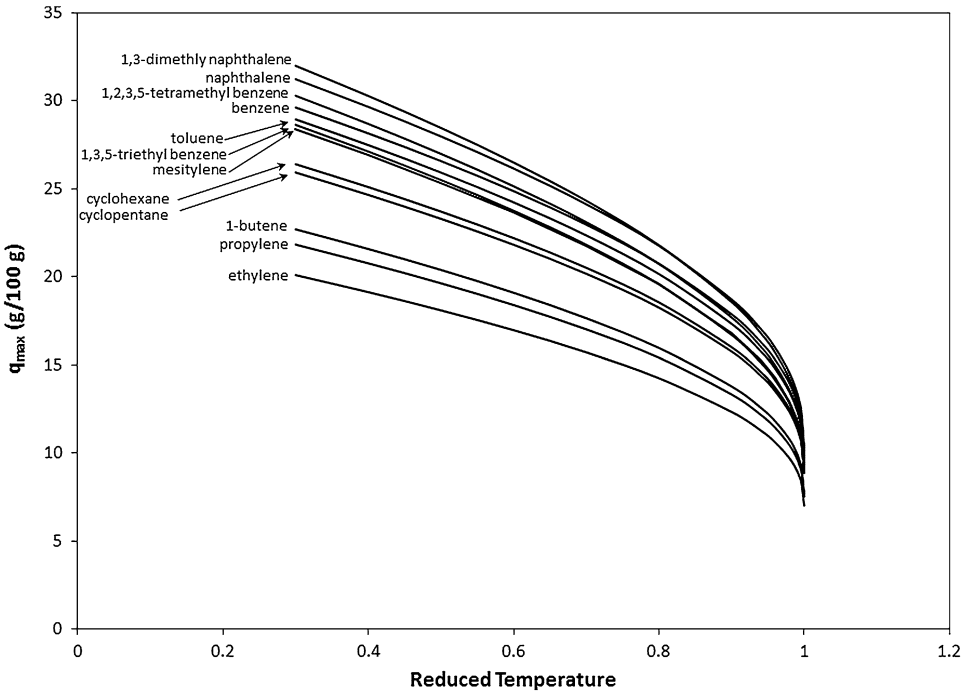

Fig. 1 Model for various species

4 Results and discussion

We begin with an assessment of the data quality for each substance. All the isotherms are plotted in supplementary data denoted by symbol S. Critical isotherms are retained in the manuscript. Also, we have installed a vertical dashed line on log–log graphs at the reduced pressure where all subcritical isotherms appear to have reached saturation. The location of this vertical line is slightly subjective but it does produce an interesting conclusion at the end of the manuscript.

Adsorption isotherms for ethylene without any modification are plotted in Fig. S2a. The original data are extracted from the respective papers summarized in Table 1. Data from four different studies, Costa et al. (1991), Danner and Choi (1978), Hyun and Danner (1982) and Narin, et al. (2014) are included ranging from a T_r of 0.99–1.50. The isotherms exhibit two patterns. All the isotherms except Narin et al. are consistent in shape but not in position. The isotherms at a T_r of 0.99 and 1.04 are levelling off too soon at high loading compared to the remaining data. This suggests an additivity of data errors in a constant volume experiment. However, it will result in a q_{max} value that is too low. The isotherm at T_r of 1.06 of Hyun and Danner and T_r of 1.04 of Costa et al. differ at the low loadings but are consistent at the high loadings. It is difficult to tell which is correct; hence, both are retained. Further, the T_r of 1.09 isotherm of Costa et al. crosses the $T_r = 1.14$ isotherms of Hyun and Danner and Danner and Choi at low loadings but appears consistent at high loadings. The implications are that the q_{max} values may be reasonable but that the Henry constants may differ. The Narin et al. isotherms appear to plateau higher from the others but as it is difficult to tell which are correct they are retained.

The isotherms are plotted on a log–log plot in Fig. S2b. In this plot, the $T_r = 1.04$ isotherm of Costa et al. looks out of position relative to its neighbors at low loading but appears reasonable at high loading. As per the criteria for choosing the saturation loading from the experimental data, the isotherm from Hyun and Danner (1982) at a T_r of 1.32 and from Narin et al. at a T_r of 1.50 are far from saturation and hence are excluded from the saturation observations. All other isotherms are leveling off and hence appear saturated. Again the Narin et al. isotherms q_{max} appears higher than the other studies. This is evident from ethylene isotherms plotted on a logarithmic scale. The isotherms with a T_r of 1.04 or greater appear to have a $(\partial \ln q)/(\partial \ln p)$ slope of 1 at low loadings consistent with Henry law, although there are slight kinks in two of the isotherms in this region. A dashed line at $P_r = 0.02$ is an approximation of the reduced pressure at which the lone subcritical isotherm has achieved saturation.

Adsorption isotherms for propylene without any modification are plotted in Figs. 2a and S3a. The original data are extracted from the respective papers summarized in Table 1. Data from six different studies, Campo et al. (2013), Costa et al. (1991), Da Silva and Rodrigues (1999), Lamia et al. (2007), van Miltenburg et al. (2008) and Narin, et al. (2014) are included ranging from a T_r of 0.76 to 1.30.

Table 1 Studies reporting adsorption of unsaturated or cyclic hydrocarbons onto 13X Zeolite

Source	Isotherm reduced temperature	Comment
Barrer et al. (1957)	Benzene: 0.53, 0.54, 0.56, 0.57, 0.59, 0.61 Toluene: 0.53, 0.54, 0.56, 0.58, 0.60 Cyclopentane: 0.58, 0.59, 0.61, 0.63, 0.65, 0.67 Cyclohexane: 0.56, 0.58, 0.60, 0.62, 0.64	Isotherms plotted on a hydrated basis have been corrected to a dehydrated basis per the % hydration indicated in the paper
Campo et al. (2013)	Propylene: 0.88, 1.02, 1.16	11 % binder, and a "better management of the dehydration process during the manufacturing of the zeolite"
Costa et al. (1991)	Ethylene: 0.99, 1.04, 1.09 Propylene: 0.76, 0.80, 0.84	Union carbide pellets, 20 % binder
Da Silva and Rodrigues (1999)	Propylene: 0.83, 0.88, 0.94, 1.02, 1.16, 1.30	CECA France pellets, 17 % binder
Danner and Choi (1978)	Ethylene: 1.06, 1.14	Linde pellets, 20 % binder
Hyun and Danner (1982)	Ethylene: 1.06, 1.14, 1.32	Union carbide pellets, 20 % binder
Kang et al. (2005)	Benzene: 0.53	Aldrich company. Deleted because percentage binder is not available
Lamia et al. (2007)	Propylene: 0.91, 0.97, 1.02, 1.08	CECA France pellets, 17 % binder
Lamia et al. (2009)	1-Butene: 0.79, 0.84, 0.89, 0.94	CECA France pellets, 17 % binder
Narin et al. (2014)	Ethylene: 1.14, 1.32, 1.50 Propylene: 0.88, 1.02, 1.16	Chemiewerk bad Köstritz GmbH binderless beads, 0 % binder
Pinto et al. (2005)	Toluene: 0.50	Molecular sieve from BDH, 20 % binder
Ruthven and Doetsch (1976)	Benzene: 0.78, 0.81, 0.87, 0.91 Toluene: 0.77, 0.82, 0.87 Cyclohexane: 0.74, 0.79, 0.83, 0.88	Union carbide crystal
Ruthven and Kaul (1993)	Mesitylene: 0.63, 0.70, 0.87, 0.90, 0.94 Naphthalene: 0.63, 0.70, 0.73, 0.77, 0.81, 0.83 1,2,3,5-tetramethylbenzene: 0.81, 0.85, 0.90, 0.94 1,3,5-Triethylbenzene: 0.85, 0.89, 0.93, 0.96 1,3-dimethylnaphthalene: 0.75	Union carbide crystal
Tezel and Ruthven (1990)	Benzene: 0.72	Union carbide crystal
van Miltenburg et al. (2008)	Propylene: 0.87, 0.98, 1.11	Synthesized new 13X zeolite using a modified recipe
Wang et al. (2004)	Benzene: 0.53 o-Xylene: 0.47 m-Xylene: 0.48 p-Xylene: 0.48	Lancaster synthesis company. Deleted because percentage binder is not available
Zhdanov et al. (1962)	Benzene: 0.53	Union carbide pellets, 20 % binder

The isotherms of Campo et al. (2013), van Miltenburg et al. (2008) and Narin et al. (2014) are significantly greater than all the other isotherms at high loading. The isotherms from these three studies agree with each other, but not with the other three studies. So, the six studies are divided into two separate groups as it is impossible to evaluate which group of studies are correct.

Propylene isotherms from Costa et al. (1991), Da Silva and Rodrigues (1999) and Lamia et al. (2007) appear consistent with one another and are plotted in Fig. S3b. The isotherms are reasonably consistent in shape and position with the exception of the $T_r = 0.83$ isotherm which appears too high, crosses other isotherms and so is deleted. Some of the isotherms are slightly out of position, but they are all retained as it is difficult to determine the accurate one. The lowest point of the $T_r = 0.91$ isotherm and the $T_r = 1.02$ isotherm, shown in grey, appears out of position and is deleted. The two lowest points for the $T_r = 1.30$ isotherm are deleted because they are out of place in the log–log plot.

Propylene isotherms from Campo et al. (2013), van Miltenburg et al. (2008) and Narin et al. (2014) are plotted in Fig. S3c. These isotherms all appear to be consistent with each other and are all retained.

The isotherms of Fig. S3b are plotted on a log–log plot in Figs. 2b and S3d. As per the criteria for choosing the

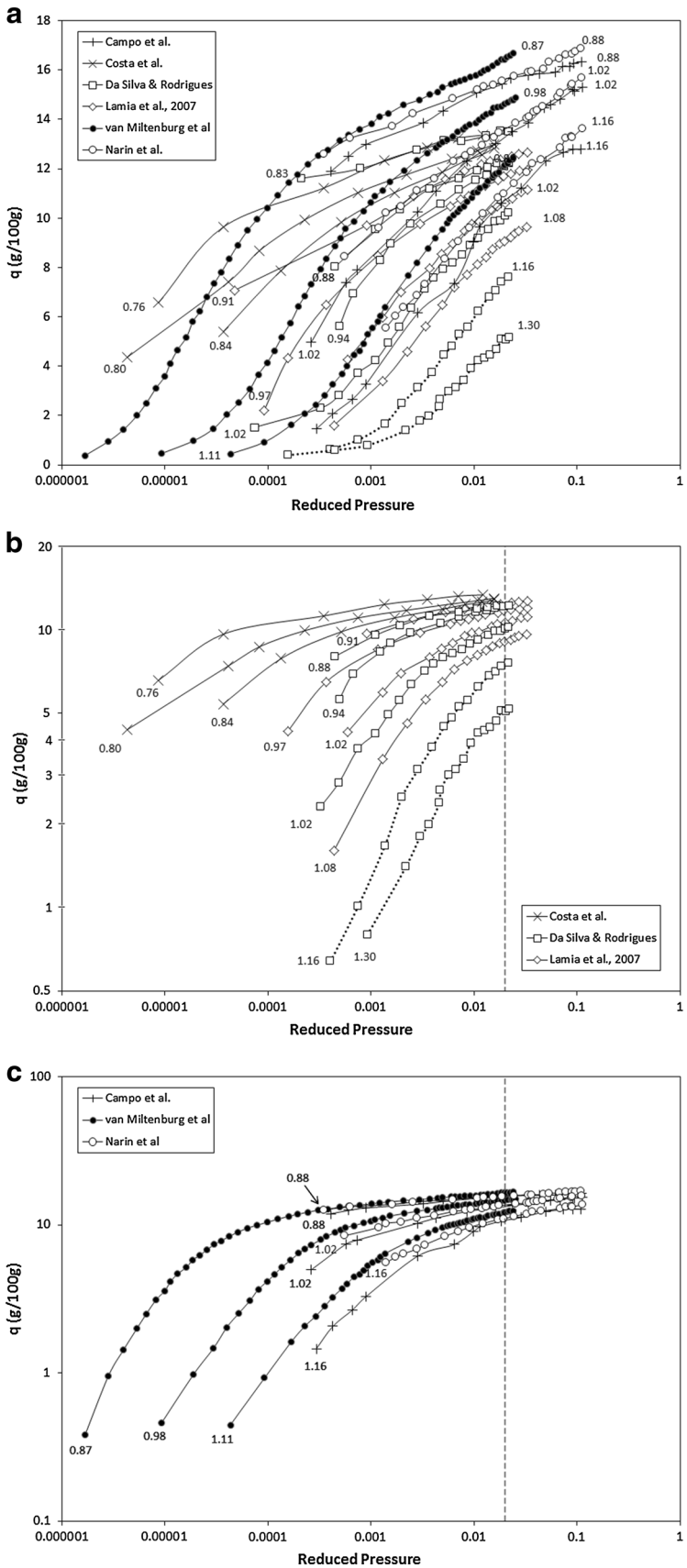

Fig. 2 **a** Propylene isotherms before screening. Reduced temperatures are indicated as *labels*. Isotherms that attain saturation have an *unbroken line*. Isotherms that have not attained or approached saturation have a *dotted line*. **b** Log–log plot of propylene from Costa et al. (1991), Da Silva and Rodrigues (1999) and Lamia et al. (2007) after screening. Reduced temperatures are indicated as *labels*. Isotherms that attain saturation have an *unbroken line*. Isotherms that have not attained or approached saturation have a *dotted line*. A *dashed line* at $P_r = 0.02$ is an approximation of the reduced pressure at which all subcritical isotherms have achieved saturation. **c** Log–log plot of propylene isotherms from Campo et al. (2013), Narin et al. (2014) and van Miltenburg et al. (2008) after screening. Reduced temperatures are indicated as *labels*. All isotherms have attained saturation. A *dashed line* at $P_r = 0.02$ is an approximation of the reduced pressure at which all subcritical isotherms have achieved saturation

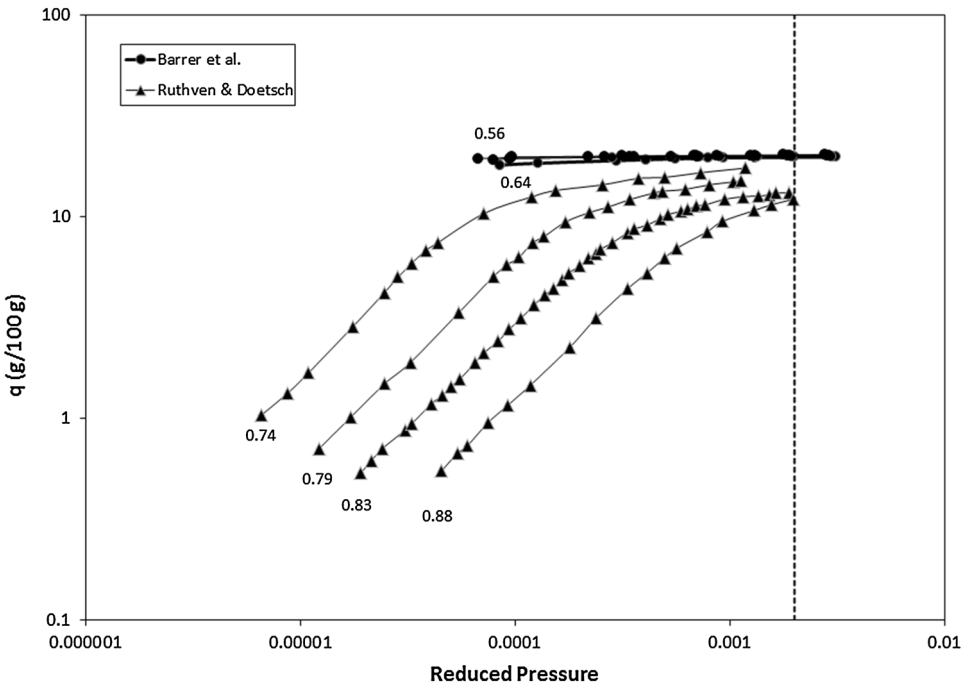

Fig. 3 Log–log plot of cyclohexane isotherms after screening. Reduced temperatures are indicated as *labels*. All isotherms have attained saturation. A *dashed line* at $P_r = 0.02$ is an approximation of the reduced pressure at which all subcritical isotherms have achieved saturation

saturation loading from the experimental data, the isotherms at T_r of 1.16 and 1.30 are far from saturation and hence are excluded from the saturation observations. All other isotherms are leveling off and hence appear saturated. The five isotherms with a T_r of 1.02 or greater appear to have a $(\partial \ln q)/(\partial \ln p)$ slope of 1 at low loadings consistent with Henry's law. A dashed line at $P_r = 0.02$ is an approximation of the reduced pressure at which all subcritical isotherms have achieved saturation.

The isotherms of Fig. S3c are plotted on a log–log plot in Figs. 2c and S3e. All these isotherms appear to meet the criteria for choosing the saturation loading. Further, the isotherms with $T_r = 0.87$, 0.98, 1.11 and 1.16 appear to have a $(\partial \ln q)/(\partial \ln p)$ slope of 1 at low loadings consistent with Henry's law. A dashed line at $P_r = 0.02$ is an approximation of the reduced pressure at which all subcritical isotherms have achieved saturation.

Adsorption isotherms for 1-butene without any modification are plotted in Fig. S4a. The original data are extracted from the paper of Lamia et al. (2008). The data range from a T_r of 0.79 to 0.94 As it is a single study, the isotherms are reasonably consistent in shape and position. The top two points of the $T_r = 0.79$ isotherm appear to exhibit capillary condensation and are deleted.

The isotherms are plotted on a log–log plot in Fig. S4b. As per the criteria for choosing the saturation loading from the experimental data, all the isotherms are leveling off and hence appear saturated. None of the isotherms extend into the Henry's law region.

Adsorption isotherms for cyclopentane without any modification are plotted in Fig. S5a. The original data are extracted from the paper of (Barrer et al. 1957). The data range from a T_r of 0.58 to 0.67. As it is a single study, the isotherms are reasonably consistent in shape and position. All data points are retained as no capillary condensation is observed.

The isotherms are plotted on a log–log plot in Fig. S5b. As per the criteria for choosing the saturation loading from the experimental data, all the isotherms are leveling off and hence appear saturated. None of the isotherms extend into the Henry law region.

Adsorption isotherms for cyclohexane without any modification are plotted in Fig. S6a. The original data are extracted from two studies (Barrer et al. 1957) and Ruthven and Doetsch (1976). The data range from a T_r of 0.56 to 0.88. The Barrer et al. data are at high loading whereas the data of Ruthven and Doetsch appear to cover the entire loading spectrum. Neither study intersects the other; so no conclusions may be drawn about the accuracy of either study. All data points are retained as no capillary condensation is observed.

The isotherms of cyclohexane are plotted on a log–log plot in Figs. 3 and S6b. As per the criteria for choosing the saturation loading from the experimental data, all the isotherms are leveling off and hence appear saturated. The four isotherms of Ruthven and Doetsch have low loadings with a $(\partial \ln q)/(\partial \ln p)$ slope of 1 consistent with Henry's law. A dashed line at $P_r = 0.02$ is an approximation of the reduced pressure at which all subcritical isotherms have achieved saturation.

Adsorption isotherms for benzene without any modification are plotted in Figs. 4a and S7a. The original data are

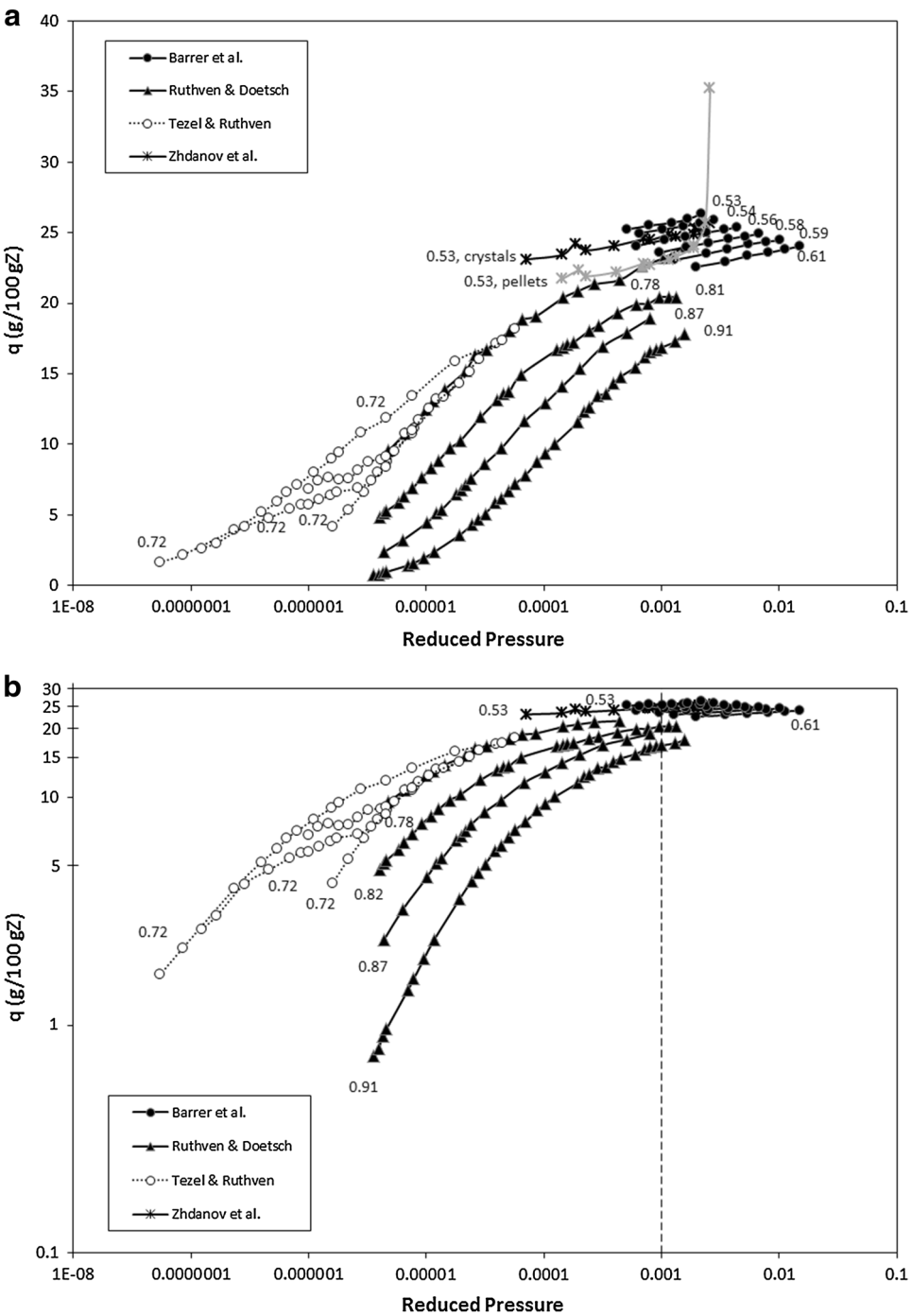

Fig. 4 **a** Benzene isotherms before screening. Reduced temperatures are indicated as *labels*. Isotherms in *grey* are inconsistent with others, and so are screened out. Isotherms that attain saturation have an *unbroken line*. Isotherms that have not attained or approached saturation have a *dotted line*. **b** Log–log plot of benzene isotherms after screening. Reduced temperatures are indicated as *labels*. Isotherms that attain saturation have an *unbroken line*. Isotherms that have not attained or approached saturation have a *dotted line*. A *dashed line* at $P_r = 0.001$ is an approximation of the reduced pressure at which all subcritical isotherms have achieved saturation

extracted from the respective papers summarized in Table 1. Data from four different studies, Barrer et al. (1957), Zhdanov et al. (1962), Ruthven and Doetsch (1976) and Tezel and Ruthven (1990) are included ranging from a T_r of 0.53 to 0.91. Zhdanov et al. measured benzene isotherms on 13X crystals and on Linde 13X pellets at a $T_r = 0.53$. The pelleted isotherm, corrected for binder, is significantly less than the crystal isotherm, and exhibits capillary condensation. The isotherm is deleted as it is significantly below the 0.53 isotherm of Barrer et al. The four isotherms of Tezel and Ruthven at $T_r = 0.72$ exhibit hysteresis. They are shown as dotted lines with open circles on the plot. The isotherms do not appear to be out of position when compared to the 0.78 isotherm, and so are retained. The six isotherms of Barrer et al. and the four isotherms of Ruthven and Doetsch are in separate regions of the graph. The $T_r = 0.78$ isotherm of Ruthven and Doetsch is the only isotherm that intercepts the Barrer et al.

isotherm; it also appears high relative to the Barrer et al. isotherms. It is difficult to ascertain which set of isotherms are correct; accordingly, they are all retained.

The isotherms of benzene are plotted on a log–log plot in Figs. 4b and S7b. Excluding the Tezel and Ruthven hysteresis isotherms, all the remaining isotherms are leveling off and hence appear to satisfy the saturation criteria. The four isotherms of Ruthven and Doetsch have low loadings with a $(\partial \ln q)/(\partial \ln p)$ slope of 1 consistent with Henry law. None of Barrer et al's isotherms are in this region. A dashed line at $P_r = 0.001$ is an approximation of the reduced pressure at which all subcritical isotherms have achieved saturation.

Adsorption isotherms for toluene without any modification are plotted in Fig. S8a. Data from three different studies, Barrer et al. (1957), Pinto et al. (2005) and Ruthven and Doetsch (1976) are included ranging from a T_r of 0.50 to 0.87. The $T_r = 0.50$ isotherm of Pinto et al. is much lower than the Barrer et al. isotherms which have T_r's between 0.53 and 0.60. It is not clear which is correct and so we have retained both sets of isotherms. As is observed for benzene, the studies of Barrer et al. and Ruthven and Doetsch are in separate regions of the graph, and do not intersect each other. Both studies are retained.

The isotherms of toluene are plotted on a log–log plot in Fig. S8b. As per the criteria, all the isotherms are leveling off and hence appear to satisfy the saturation criteria. Only the $T_r = 0.82$ and 0.87 isotherms of Ruthven and Doetsch have a low loading with a $(\partial \ln q)/(\partial \ln p)$ slope of 1 consistent with Henry's law. Neither Pinto et al. isotherm nor Barrer et al's isotherms are in this region. A dashed line at $P_r = 0.003$ is an approximation of the reduced pressure at which all subcritical isotherms have achieved saturation.

Ruthven and Kaul performed a comprehensive study of five large molecular weight aromatic species. The isotherms are displayed in Fig. S9a in subplots i–v. As all the isotherms are from a single study, the isotherms are reasonably consistent in shape and position Adsorption isotherms for mesitylene without any modification are plotted in Fig. S9a subplot i. The data range from a T_r of 0.63 to 0.94. One isotherm at $T_r = 0.87$ does not approach saturation. Adsorption isotherms for naphthalene without any modification are plotted in Fig. S9a subplot ii. The data range from a T_r of 0.63 to 0.83. Four isotherms in the T_r range of 0.73 to 0.83 do not approach saturation. Adsorption isotherms for 1,2,3,5-tetramethylbenzene without any modification are plotted in Fig. S9a subplot iii. The authors measured isotherms for this species on both 2 and 50 micron crystal particles. We use only the 2 micron data, as the 50 micron data did not reach equilibrium. The data range from a T_r of 0.81 to 0.94. One isotherm at $T_r = 0.94$ does not approach saturation. Adsorption isotherms for 1,3,5-triethylbenzene without any modification are plotted in Fig. S9a subplot iv. As for 1,2,3,5-tetramethylbenzene, we use only the 2 micron data, as the 50 micron data did not reach equilibrium. The data range from a T_r of 0.85 to 0.96. Two isotherms at $T_r = 0.93$ and 0.96 do not approach saturation. One adsorption isotherm for 1,3-dimethylnaphthalene is plotted in Fig. S9a subplot v for a T_r of 0.75.

Isotherms for the five species are plotted on log–log plots in Fig. S9b in five subplots. As per the criteria for choosing the saturation loading from the experimental data, isotherms that are leveling off and hence appear saturated are shown with a solid line. Isotherms that have not attained or approach saturation have a dotted line. Several isotherms extend into the Henry's Law region: four of the mesitylene isotherms from $T_r = 0.87$ to $T_r = 0.94$, five of the naphthalene isotherms from $T_r = 0.70$ to 0.83, two of the 1,2,3,5-tetramethylbenzene isotherms at $T_r = 0.90$ and 0.94, four of 1,3,5-triethylbenzene isotherms at $T_r = 0.85$, 0.89, 0.93 and 0.96, and the single isotherm of 1,3-dimethylnaphthalene at T_r of 0.75 extend into the Henry's law region. Dashed lines for mesitylene, 1,2,3,-tetraethlbenzene, and 1,3-dimethylnaphthalene at $P_r = 6 \times 10^{-5}$, 2×10^{-5}, and 8×10^{-7} respectively, are approximations of the reduced pressures at which all subcritical isotherms have achieved saturation.

An interesting observation is how, for a given species, the subcritical isotherms all tend to reach saturation at approximately the same pressure as shown by the vertical dashed lines in the log–log Figures. This was previously noted for subcritical alkanes on 5A zeolite in Loughlin and Abouelnasr (2009); the reduced pressure at which most alkanes reached saturation for subcritical isotherms was reported to be around 0.03. A similar value, around 0.02, can be observed in the isotherms for alkanes on 13X (Al Mousa et al. 2014), and also for alkenes on 13X in this study. However, as the molecular weight increases, the reduced pressure at which this occurs decreases. Estimates of this value for both 13X and 5A zeolites are plotted versus molecular weight in Figs. 5 and S10. There is a remarkable similarity between the different adsorbent/adsorbate systems, except for one outlier, dodecane on 5A. A threshold molecular weight of 60 g/mol becomes apparent. Species with MW's below this threshold have a subcritical saturation P_r around 0.01–0.03. For species with MW's above 60 g/mol, the subcritical saturation P_r decreases exponentially with increasing MW. A fit of the data for 13X species is shown in Fig. 5. Using this correlation for example, the addition of a methyl group (MW = 15), would result in a decrease in the subcritical saturation P_r by a factor of 5 on 13X zeolite.

The maximum saturation concentrations for all the species are plotted in Figs. 6 and S11 as q_{max} versus T_r. The cycloalkanes plot is illustrated in Fig. 6i. The maximum concentrations are shown as data points and the theoretical predictions as curves for cyclopentane and

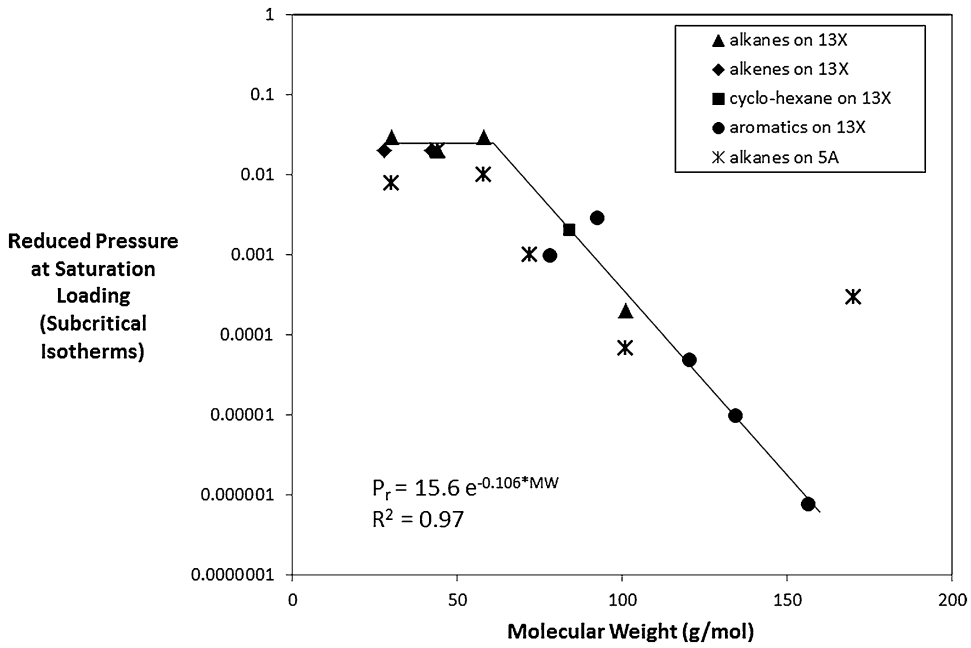

Fig. 5 Subcritical saturation reduced pressure versus molecular weight for several adsorbate/adsorbent systems

cyclohexane respectively. The data points for cyclopentane (Δ) of Barrer et al. cross the predicted plots whereas those for cyclohexane (○) of Barrer et al. and Ruthven and Doetsch are below the predictions. In our earlier study (Al Mousa et al. 2014) we reported that the data of Barrer et al. appeared to be too high. The results for cyclopentane are consistent with this observation. Further the results for cyclohexane indicate that Barrer et al's. data points, the top four (○), are closer to the predicted plot than those of Ruthven and Doetsch, the bottom four (○), which suggests that they may be a little too high.

The alkenes plot, illustrated in Fig. 6ii, is separated into two regions, a subcritical region to the left below $T_r = 1$ and a supercritical region to the right above $T_r = 1$. The data in the subcritical region, comprising propylene and 1-butene, lie between the predicted saturation loadings for propylene and 1-butene, indicated by the solid lines in the Figure. However, the data for propylene exhibit a dichotomy. The data for Fig. 2b fits the theoretical relationship but that for Fig. 2c does not. This data is for the study of Campo et al., van Miltenburg et al. and Narin et al. The latter three studies are for 13X zeolite prepared with new recipes. It is unclear whether these 13X zeolites are the same as the other studies. The data in the subcritical region for either species demonstrate the same shape as illustrated in Fig. 1 for the theoretical calculation for q_{max}. The data in the supercritical region, comprising ethylene, propylene and 1-butene, lie between two bounding lines at $q_{max} = 8$ and 12 g/100 g. There is no consistent pattern to the experimental data in this region; hence the use of a fixed range of

$$q_{max} = 10 \pm 2\,\mathrm{g}/100\,\mathrm{g} \quad (6)$$

may be appropriate for the supercritical region. This is similar to, although a little higher than the observation made for supercritical alkanes on 5A or 13X zeolite (Loughlin and Abouelnasr 2009; Al Mousa et al. 2014).

The aromatics plot is illustrated in Fig. 6iii. The maximum concentrations are shown as data points and the theoretical predictions as curves for mesitylene and 1,3-dimethyl napthalene respectively, the outer limits of the aromatics curves. The benzene-toluene data of Barrer et al. falls between the two curves whereas the toluene data of Pinto et al. and Ruthven and Doetsch (1976) falls below the predicted curves. This supports the observation made earlier that the Barrer et al. results may be too high. The remaining compounds, basically benzene rings with methyl groups attached (as is toluene) fall significantly below the predicted curves. This indicates that the attached methyl groups are causing steric factor complications resulting in incomplete filling of the cavities for these compounds.

The observed data are also plotted as a normalized parameter Γ, calculated using Eq. 4, versus T_r in Figs. 7 and S12. The model is represented as a solid line in the Figure, and is defined by Eq. 3. The observations made for q_{max} versus T_r in Fig. 6i, ii and iii are equally applicable for these Figures.

The data and predictions in Fig. 7iii disagree. In an effort to improve the predictions, the data is regressed using the steric factor Eq. 5. The steric factors are only applied to data points with T_r between 0.65 and 1.00. A constraint is made that no data point that was originally below the Γ-curve could go above it when the steric factor is applied. The calculated optimum steric factors are presented in

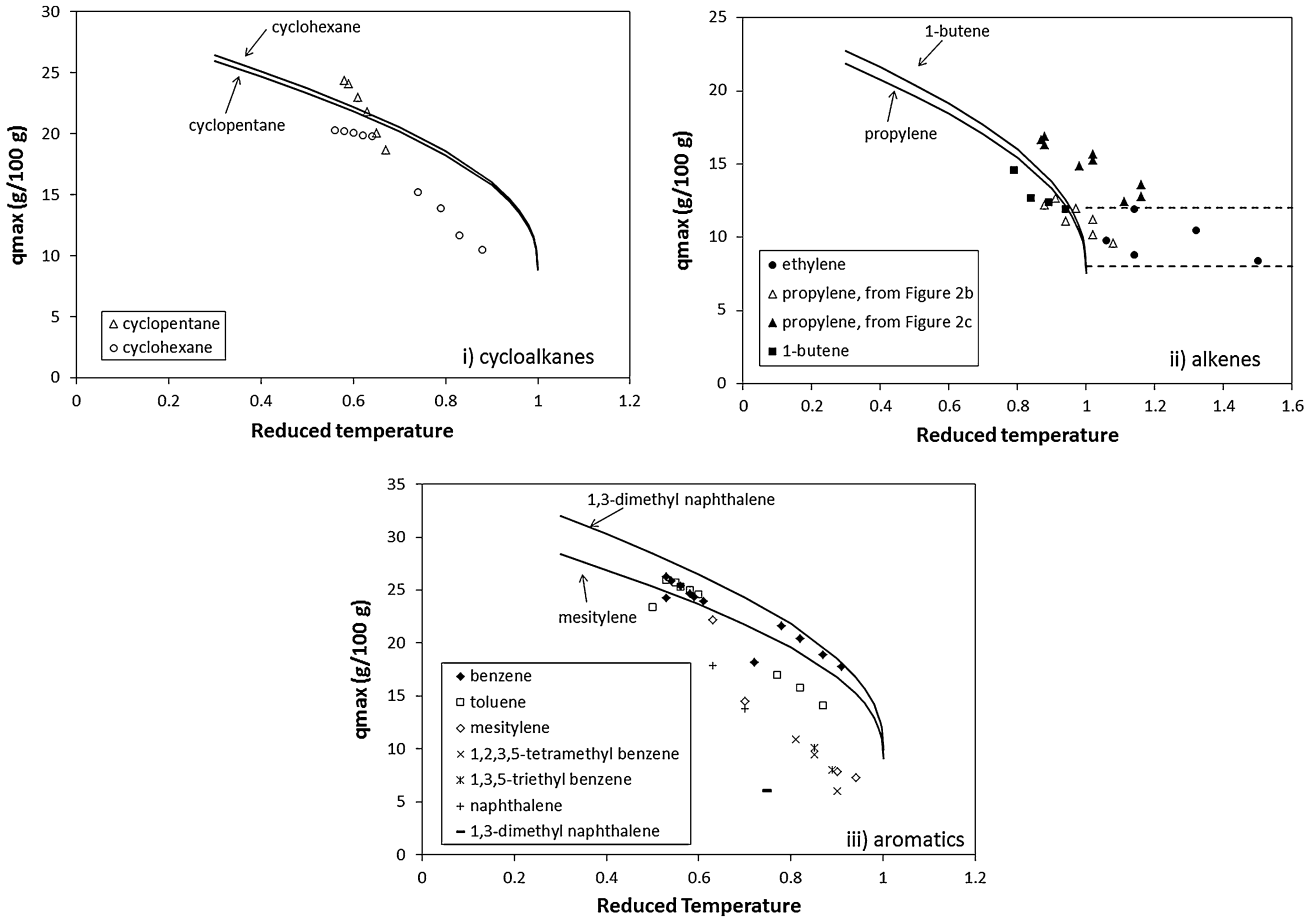

Fig. 6 q_{max} versus T_r for all **i** cyclo-alkanes; **ii** alkenes; and **iii** aromatic species. *Bounding-lines* for supercritical adsorption are at 8 and 12 g/100 g

Table 2 and plotted in Figs. 8 and S13 versus molecular weight. The data is reasonably linear versus molecular weight. The data are regressed giving

$$\lambda = -0.0067MW + 1.482 \quad (7)$$

with a correlation coefficient of 0.791. This indicates that about 0.67 % of the zeolite void volume becomes inaccessible for every added gram in the molecular weight for large molecules. Another way to visualize this is that for every additional methyl group (MW = 15 g/mol), another 10 % of the void volume becomes inaccessible through steric effects. The revised gamma plot employing these steric factors is presented in Figs. 9 and S14. As may be observed, Fig. 9 is a big improvement over Fig. 7iii.

5 Conclusions

The published experimental adsorption isotherms of unsaturated and cyclic hydrocarbons in 13X zeolite are evaluated for consistency using semi-log plots of the isotherms for each species. Several studies are found to be relatively consistent for four of the species. Eight other species are reported by only one study. The isotherms are then evaluated to determine whether they attained or approached saturation using log–log plots of the isotherms. The maximum experimental adsorption of those isotherms at or near saturation is recorded.

The experimental data fall into two regions, a subcritical region and a supercritical region. In the subcritical region, the reduced pressure at which all isotherms are saturated is observed to be constant at 0.02 for substances with a molecular weight of 60 g/mol or less, and then decreases exponentially with molecular weight above 60 g/mol. Also in the subcritical region, the model proposed in our earlier papers (Loughlin and Abouelnasr 2009; Al Mousa et al. 2014) for saturation loading using the modified Rackett equation of Spencer and Danner (1972) for saturated liquid densities combined with crystallographic data for the 13X zeolite is used. The maximum experimental adsorption for cyclo alkanes and for alkenes are consistent with the proposed model. Steric factors are required for aromatic

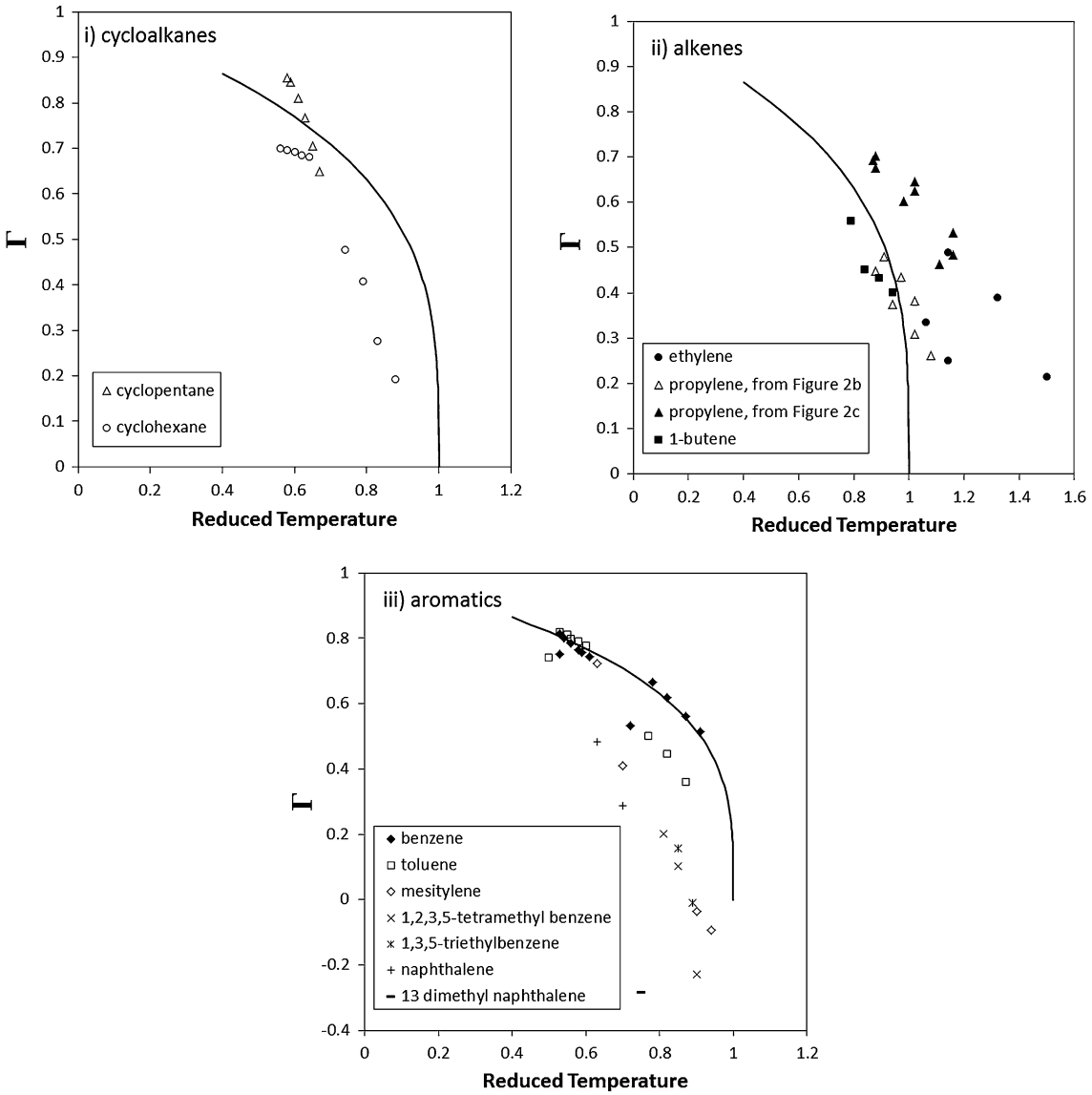

Fig. 7 Normalized parameter, Γ (from Eq. 4) versus reduced temperature for **i** cyclo-alkanes; **ii** alkenes; and **iii** aromatic species. The *solid line* is the theoretical plot of normalized parameter Γ* against reduced temperature, Eq. 3

Table 2 Steric factors for aromatic species. Note that steric factors are only applied to $T_r > 0.65$, and any data point originally below the gamma line is forced to stay on or below the gamma line

Species	MW (g/mol)	Steric factor
Benzene	78	1
Toluene	92	0.815
Mesitylene	120	0.665
Naphthalene	128	0.7
1,2,3,5-tetramethylbenzene	134	0.56
1,3,5-triethylbenzene	162	0.55
1,3-dimethylnaphthalene	156	0.26

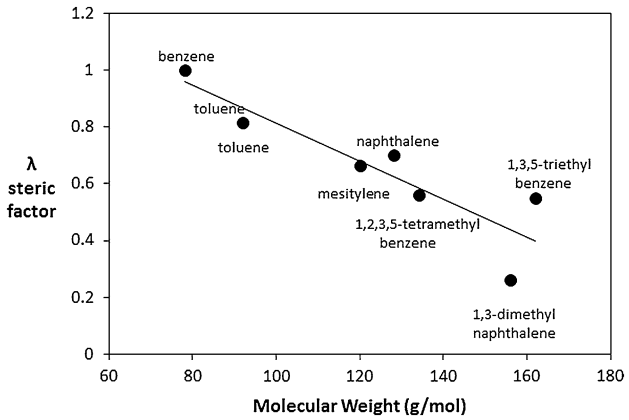

Fig. 8 Steric factors versus molecular weight

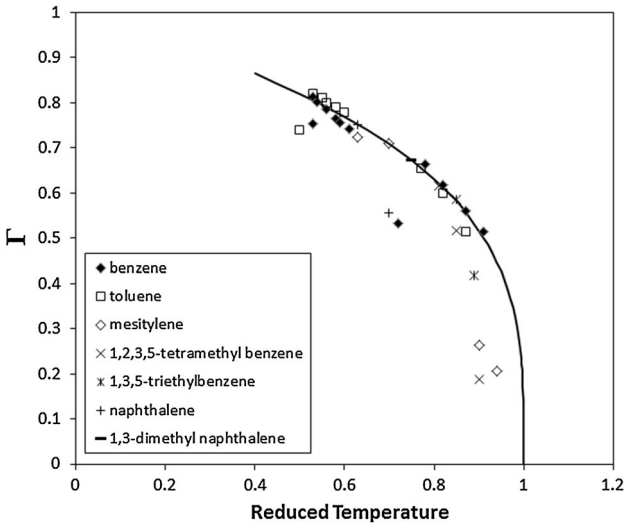

Fig. 9 Gamma plot for aromatics after compensating with the steric factor

species; the steric factor is negatively correlated with the molecular weight of the adsorbate. In the supercritical region only alkene data are available; and the saturation loading is ill defined. A correlation equation of $q_{max} = 10. \pm 2.0$ g/100 g satisfactorily fits the data. The use of the upper bound of 12 g/100 g is recommended in the absence of sufficient data.

Acknowledgments The authors wish to acknowledge the support of the American University of Sharjah and the California State University at Bakersfield during this study.

References

Al Mousa, A., Abouelnasr, D., Loughlin, K.: Saturation loadings on 13X (faujasite) zeolite above and below the critical conditions. Part I: alkane hydrocarbons data evaluation and modelling. Adsorption (2015). doi:10.1007/s10450-015-9672-x

Barrer, R.M., Bultitude, F.W., Sutherland, J.W.: Structure of faujasite and properties of its inclusion complexes with hydrocarbons. Trans. Faraday Soc. **53**, 1111–1123 (1957)

Breck, D.: Zeolite Molecular Sieves; Structure, Chemistry and Use. Wiley, New York (1974)

Campo, M., Riberio, A., Ferreira, A., Santos, J., Lutz, C., Loueiro, J.A.: New 13X zeolite for propylene/propane separation by vacuum swing adsorption. Sep. Purif. Technol. **103**, 60–70 (2013)

CHERIC. (Accessed 2012). Retrieved from http://www.cheric.org/kdb/research/hcprop/cmpsrch.phpe

Costa, E., Calleja, G., Jimenez, A., Pau, J.: Adsorption equilibrium of ethylene, propane, propylene, carbon dioxide, and their mixtures on 13X zeolite. J. Chem. Eng. Data **36**(2), 218–224 (1991)

Da Silva, F., Rodrigues, A.: Adsorption equilibria and kinetics for propylene and propane over 13X and 4A zeolite pellets. Ind. Eng. Chem. Res. **38**(5), 2051–2057 (1999)

Danner, R.P., Choi, E.C.: Mixture adsorption equilibria of ethane and ethylene on 13X molecular sieves. Ind. Eng. Chem. Fundam. **17**(4), 248–253 (1978)

Hyun, S., Danner, R.P.: Equilibrium adsorption of ethane, ethylene, isobutane, carbon dioxide, and their binary mixtures on 13X molecular sieves. J. Eng. Chem. Data **27**(2), 196–200 (1982)

Kang, S.-W., Min, B.-H., Suh, S.-S.: Determination of Adsorption Isotherm Parameters by Breakthrough Curves in Activated Carbon and Zeolite 13X Packed Bed. J. Korean Ind. Eng. Chem. **16**(1), 131–138 (2005)

Lamia, N., Granato, M.A., Sa Gomes, P., Grande, C.A., Wolff, L., Leflaive, P., Rodrigues, A.E.: Propane/propylene separation by simulated moving bed II. Measurement and prediction of binary adsorption equilibria of propane, propylene, isobutane and 1-butene on 13X zeolite. Sep. Sci. Technol. **44**(7), 1485–1509 (2009)

Lamia, N., Wolff, L., Leflaive, P., Sa Gomes, P.: Propane/propylene separation by simulated moving bed I Adsorption of propane, propylene and isobutane in pellets of 13X zeolite. Sep. Sci. Technol. **42**(12), 2539–2566 (2007)

Lamia, N., Wolff, L., Leflaive, P., Leinekugel-Le-Cocq, D., Sá Gomes, P., Grande, C.A., Rodrigues, A.E.: Equilibrium and fixed bed adsorption of 1-butene, propylene and propane over 13X zeolite pellets. Sep. Sci. Technol. **43**(5), 1124–1156 (2008)

Loughlin, K.F., Abouelnasr, D.M.: Sorbate densities on 5A zeolite above and below the critical conditions: n alkane data evaluation and modeling. Adsorption **15**, 521–533 (2009)

Narin, G., Martins, V., Campo, M., Ribeiro, A., Ferreira, A., Santos, J., Schumann, K., Rodrigues, A.E.: Light olefins/paraffins separation with 13X zeolite binderless beads. Sep. Purif. Technol. **133**, 452–475 (2014)

Pinto, M.L., Pires, J., Carvalho, A.P., de Carvalho, M.B., Bordado, J.C.: Characterization of adsorbent materials supported on polyurethane foams by nitrogen and toluene adsorption. Microporous Mesoporous Mater. **80**(1), 253–262 (2005)

Ruthven, D.M., Kaul, B.K.: Adsorption of aromatic hydrocarbons in NaX zeolite. 1. Equilibrium. Ind. Eng. Chem. Res. **32**(9), 2047–2052 (1993)

Ruthven, D., Doetsch, I.: Diffusion of hydrocarbons in 13X Zeolite. AIChE J. **22**(5), 882–886 (1976)

Spencer, C., Danner, R.: Improved equation for prediction of saturated liquid density. J. Chem. Eng. Data **17**(2), 236–240 (1972)

Tezel, O.H., Ruthven, D.M.: Sorption of benzene in Na X zeolite: an unusual hysteresis effect. J. Colloid Interface Sci. **139**(2), 581–583 (1990)

van Miltenburg, A., Gascon, J., Zhu, W., Kapteijn, F., Moulijn, J.A.: Propylene/propane mixture adsorption on faujasite sorbents. Adsorption **14**(2–3), 309–321 (2008)

Wang, C.M., Chang, K.S., Chung, T.W., Wu, H.: Adsorption equilibria of aromatic compounds on activated carbon, silica gel, and 13X zeolite. J. Chem. Eng. Data **49**(3), 527–531 (2004)

Zhdanov, S.P., Kiselev, A.V., Pavlova, L.F.: Adsorption of benzene and n-hexane and their liquid solutions by 10X and 13X zeolites. Kinet. Katal. **3**(3), 391–394 (1962)